Influence of Model Parameters and Inlet Turbulence Boundary Specification Methods in Secondary Settling Tanks: Computational Fluid Dynamics Study

Haiwen Gao, Ph.D.[1]; and M. K. Stenstrom, Ph.D., F.ASCE[2]

Abstract: Computational fluid dynamics (CFD) has been applied in secondary settling tank (SST) analysis for more than 30 years. Although great progresses has been achieved, there are still some uncertainties in CFD SST modeling. In this study, a numerical model is used to understand the effects of two model parameters: r_p, accounting for particles with poor settling properties in the Takács settling model; and ρ_p, the dry solids density. Both parameters are used in the user-defined functions to couple solids transport on settling velocity. Also, the differences in turbulence specification methods in prediction of SST performance are evaluated. The results show that the prediction of effluent suspended solids (ESS) is very sensitive to r_p. The incorrect specification of r_p may mask real improvements in SST geometry, and may even cause clarification failure prediction under the normal inflow conditions. The value of ρ_p has less impact on ESS prediction, and its specification is less critical to maintain ESS prediction consistently with field data. Neither return activated sludge concentration (RAS) nor sludge blanket height (SBH) is sensitive to the effects of r_p and ρ_p. Additionally, the initial turbulent kinetic energy and turbulent dissipation rate specification methods produce only local effects on the hydrodynamics near the inlet boundary, and none of the performance indicators (ESS, RAS, or SBH) are sensitive to inlet boundary turbulence specification methods. **DOI: 10.1061/(ASCE)EE.1943-7870.0001689.**

Author keywords: Secondary settling tank; Computational fluid dynamics; Takács settling model; Dry solids density; Inlet turbulence specification.

Introduction

In conventional wastewater treatment plants (WWTPs), secondary settling tanks (SSTs)—also known as secondary sedimentation tanks or secondary clarifiers—are used in the activated sludge process (ASP) to remove organic matter and reduce nutrients such as nitrogen and phosphorus (Li and Stenstrom 2014). SST performance is important for overall plant efficiency, and techniques to improve performance have been evaluated and modeled using computational fluid dynamics (CFD), especially with the availability of greater computing resources. Since Larsen (1977) set the framework for CFD modeling of settling tanks, CFD has become a popular tool for researchers and engineers to understand the hydrodynamics of SSTs and to optimize their internal geometry and process efficiency (Zhou and McCorquodale 1992a, b, c; Samstag et al. 1992; Krebs et al. 1996; Vitasovic et al. 1997; McCorquodale et al. 2004; Xanthos et al. 2011; Patziger et al. 2012; Xanthos et al. 2013; Das et al. 2016; Patziger 2016; Gao and Stenstrom 2017).

Despite the successes in CFD modeling of SSTs, a significant shortcoming of CFD modeling is lack of a generally accepted SST modeling framework (assumptions for turbulence, settling velocity, sludge rheology). The different assumptions implemented in the model framework still do not fully conform to experimental observations, and improvements are still needed.

In the CFD modeling for SSTs, one of the major constraints is the lack of a consistent way to calculate sludge settling properties, which are needed to accurately describe clarification, settling, and compression of the sludge over the range of concentrations routinely found in SSTs (Plósz et al. 2012). Li and Stenstrom (2014), in their work on 1D SST modeling, reviewed 15 different functions of settling velocity versus concentration. Although many model improvements have been achieved based on the Takács settling equation (Takács et al. 1991; Bürger et al. 2011; Guyonvarch et al. 2015; Xu et al. 2017), they have not been widely accepted by engineers. Compared with the Takács settling model, these models have more parameters needing calibration and are time-consuming for practicing engineers. Therefore, Takács model [Eq. (1)] is still the most popular sludge settling equation being implemented in CFD SST models

$$V_s = V_o\left(e^{-r_h(C-C_{\min})} - e^{-r_p(C-C_{\min})}\right) \quad (1)$$

where V_o = Stokes velocity; and r_h and r_p account for rapidly and poorly settling floc, respectively. The constant $C_{\min}$ = concentration of unsettleable solids in the effluent of the SST (Vitasovic et al. 1997). While the value of r_h can be obtained from a series of batch tests over a concentration range by measuring the zone settling velocities as the linear descending rate of the liquid/solid interface in academic projects (Burt 2010; Ramin et al. 2014)—and can be correlated with sludge volume index (SVI), stirred sludge volume index (SSVI), and diluted sludge volume index (DSVI) in many consulting projects (Wahlberg and Keinath 1988; Daigger 1995; Griborio and McCorquodale 2016)—there is no guidance to obtain the value of r_p. Table 1 shows that differences among values of r_p used in previous studies are significant. Since Ekama and Marais

[1]Postdoctoral Researcher, Dept. of Civil and Environmental Engineering, Univ. of California Los Angeles, 6805 Boelter Hall, Los Angeles, CA 90095. ORCID: https://orcid.org/0000-0001-7387-2289. Email: haiweng92@g.ucla.edu

[2]Professor, Dept. of Civil and Environmental Engineering, Univ. of California Los Angeles, 5714 Boelter Hall, Los Angeles, CA 90095 (corresponding author). Email: stenstro@seas.ucla.edu

Note. This manuscript was submitted on May 29, 2019; approved on October 15, 2019; published online on March 5, 2020. Discussion period open until August 5, 2020; separate discussions must be submitted for individual papers. This paper is part of the ***Journal of Environmental Engineering***, © ASCE, ISSN 0733-9372.

(2004) stated that value of r_p in the Takács settling model affects the CFD prediction of ESS, its effect is quantified in this study.

The second constraint is the lack of a generally accepted sludge rheological model. Lakehal et al. (1999) and Saffarian et al. (2010, 2011) conducted sensitivity studies for previously published sludge rheological models such as the Bokil, Casson Bingham, Herschel-Bulkley, and modified Herschel-Bulkley models. The results showed that the application of different sludge rheological models has significant impacts on the prediction of concentration and velocity fields. Additionally, because there is no consensus on the comprehensive and repeatable rheological measurement procedure (Ratkovich et al. 2013), these different rheological models should be applied cautiously.

The third constraint is the applications of turbulence models. Although standard k-ε model (SKE) has been widely applied in CFD SST modeling over the last 30 years because of its robustness, economy, and reasonable accuracy for the prediction of turbulent flow in SSTs, two modified versions of SKE (RNG k-ε model and Realizable k-ε model) have been used in several recent settling tank studies (Tamayol et al. 2009; Tarpagkou and Pantokratoras 2013; Das et al. 2016; Patziger 2016). Gao and Stenstrom (2018a) compared the performance of these three turbulence models, and the results showed that the prediction difference of flow and concentration fields among these models is significant. The predicted sludge blanket height (SBH) and concentration of returned activated sludge (RAS) are more than 10% among different turbulence models.

Also, the inlet turbulence boundary condition can be specified using the estimated turbulent kinetic energy (TKE) and turbulent dissipation rate (TDR) or turbulent intensity (TI) and hydraulic diameter. Table 1 summarizes three turbulence specification methods for the inlet turbulence boundary condition. The first two methods (14 and 15) estimate the TKE and TDR at the inlet boundary, and the third method (16) uses TI and hydraulic diameter to define the turbulence profile at the inlet boundary. With the same inflow conditions and internal structure, the prediction of the inlet TKE and TDR can be more than one and two orders of magnitude among these three different turbulence specification methods. Therefore, different inlet turbulence specification methods can have strong effects on the prediction of SST performance.

Additionally, there are uncertainties in the model parameters, such as (1) the turbulent Schmidt number (σ_c) in the sludge transport equation; (2) the coupling of the buoyancy term (G_b) in the TKE equation; (3) the coefficient of the buoyancy term (C_3) in the TDR equation; and (4) the dry solids density (ρ_p). The effects of the uncertainties of the first three model parameters have been investigated previously by Gao and Stenstrom (2018b), and the effects of r_p and ρ_p are discussed in this study. Since ρ_p is coupled within every governing equation, the variation of ρ_p will influence the entire flow and concentration fields.

Table 1 shows key model parameter values and boundary conditions used in previous studies. There is a large range in values, and there is no systematic way of predicting the impact of the parameter uncertainties and different inlet turbulence boundary conditions. The hydrodynamics of the entire SST are very sensitive to the changes of the inlet boundary condition and parameters, which means it is important to understand the effects of varied conditions on SST performance.

In this study, sensitivity studies were conducted to understand the effects of the uncertainties of r_p and ρ_p, as well as the different inlet turbulence specification methods. Three different conditions, varying flow rate, solids concentration, and recycle rate for the SSTs of the Witney WWTP, described by Burt (2010), are used in the sensitivity study. Trial 1 is applied to the original circular SST, and Trials 2 and 3 are applied to the modified circular SST. The performance indicators (ESS, RAS concentration, and SBH) and the sludge settling velocity, flow, and concentration profiles are observed as a function of the different values of the model parameters. For brevity, only the trial showing the largest discrepancy between the prediction and measurement of the performance indicator are presented as the representative trial to illustrate the differences in the profiles.

Table 1. Range of key model parameters used in previous studies: Settling parameter accounting for the particle with poor settling property (r_p, Takács settling model), dry solids density (ρ_p), and turbulence specification method for the inlet boundary condition

Number	Parameters and definitions	References
		r_p (L/g)
1	4	McCorquodale et al. (2004)
2	5	McCorquodale et al. (2004)
3	10	Vitasovic et al. (1997) and Ekama and Marais (2004)
4	$10r_h$[a]	Ekama et al. (1997) and Weiss et al. (2007)
5	15–30	Zhou and McCorquodale (1992a)
6	20	Tamayol et al. (2009)
		ρ_p (kg/m^3)
7	1,100	Deininger et al. (1998)
8	1,450	Larsen (1977); Saffarian et al. (2010)
9	1,500	Tarpagkou and Pantokratoras (2013)
10	1,600	Weiss et al. (2007)
11	1,360–1,660	Zhou and McCorquodale (1992a)
12	1,700–1,800	Kinnear (2002)
13	1,907/1,743/2,070	Xu et al. (2017)
	Inlet turbulence-boundary conditions	
14	$k_{in} = 1.5(I_u v_{in})^2$ $\varepsilon = \frac{C_\mu^{\frac{3}{4}} k_{in}^{\frac{3}{2}}}{\kappa L_u}$	Lakehal et al. (1999) and Saffarian et al. (2010, 2011)
15	$k_{in} = \alpha u_o^2$ $\varepsilon = \frac{C_\mu^{\frac{3}{4}} k_{in}^{\frac{3}{2}}}{L_m}$	Zhou and McCorquodale (1992a) and Kleine and Reddy (2005)
16	TI hydraulic diameter	Gao and Stenstrom (2018a, b, 2019a, b, c, d)

[a]r_h = exponential term accounting for the particle with good settling property.

Materials and Methods

Governing Equations and Boundary Conditions

A 2D CFD SST model was developed to conduct the sensitivity tests, and provides detailed insight into the complex flow and transport processes in the SST. This method can largely reduce the number of cells and calculation time without deteriorating the accuracy of the simulation compared with the 3D simulations (Patziger 2016). The turbulent flow is modeled by the Reynolds-averaged Navier-Stokes equations with a SKE model closure (Rodi 1980). The solids transport process is calculated by user-defined advection-diffusion equation, with terms describing settling and thickening based on the Takács settling function (Takács et al. 1991; Patziger et al. 2012). All the governing equations are numerically solved by the commercial CFD code ANSYS Fluent (v.18.2) (Pittsburgh, Pennsylvania).

The equations describing 2D, steady, turbulent, and density stratified flow in a circular SST are as follows:

$$\frac{\partial ru}{\partial r} + \frac{\partial rv}{\partial y} = 0 \tag{2}$$

The r-momentum component is

$$u\frac{\partial u}{\partial r} + v\frac{\partial u}{\partial y} = -\frac{1}{\rho}\frac{\partial p}{\partial r} + \frac{1}{r}\frac{\partial}{\partial r}\left[r(\theta+\theta_t)\frac{\partial u}{\partial r}\right] + \frac{1}{r}\frac{\partial}{\partial y}\left[r(\theta+\theta_t)\frac{\partial u}{\partial y}\right] + S_u \tag{3}$$

The y-momentum component is

$$u\frac{\partial v}{\partial r} + v\frac{\partial v}{\partial y} = -\frac{1}{\rho}\frac{\partial p}{\partial y} + \frac{1}{r}\frac{\partial}{\partial r}\left[r(\theta+\theta_t)\frac{\partial v}{\partial r}\right] + \frac{1}{r}\frac{\partial}{\partial y}\left[r(\theta+\theta_t)\frac{\partial v}{\partial y}\right] - g\frac{\rho-\rho_r}{\rho} + S_v \tag{4}$$

where

$$S_u = \frac{1}{r}\frac{\partial}{\partial r}\left[r(\theta+\theta_t)\frac{\partial u}{\partial r}\right] + \frac{1}{r}\frac{\partial}{\partial y}\left[r(\theta+\theta_t)\frac{\partial v}{\partial r}\right] - 2\frac{\theta+\theta_t}{r^2} \tag{5}$$

$$S_v = \frac{1}{r}\frac{\partial}{\partial r}\left[r(\theta+\theta_t)\frac{\partial u}{\partial y}\right] + \frac{1}{r}\frac{\partial}{\partial y}\left[r(\theta+\theta_t)\frac{\partial v}{\partial y}\right] \tag{6}$$

where u and v = mean velocity components in the r (radial) and y (axial) directions, respectively; p = general pressure less the hydrostatic pressure at reference density ρ_r; ρ = density of mixture; g = acceleration of gravity; θ = viscosity of the sludge mixture; and θ_t = turbulent eddy viscosity. For density-driven flows, the local fluid density is related to the local values of the sediment concentration by the following relationship:

$$\rho = \rho_r + C\left(1 - \frac{\rho_r}{\rho_p}\right) \tag{7}$$

where C = SS concentration; ρ_p = dry particle density assumed to be 1,450 kg/m^3 (Larsen 1977); ρ_r = reference density (clear water); and ρ = density of the fluid-solid mixture.

The general transport equations for the TKE (k) and the turbulence dissipation rate (ε) of the standard k-ε turbulence model can be described by Eqs. (8) and (9), respectively, as

$$u\frac{\partial k}{\partial r} + v\frac{\partial k}{\partial y} = \frac{\partial}{\partial r}\left[\left(\theta + \frac{\theta_t}{\sigma_k}\right)\frac{\partial k}{\partial r}\right] + \frac{\partial}{\partial y}\left[\left(\theta + \frac{\theta_t}{\sigma_k}\right)\frac{\partial k}{\partial y}\right] + G_k + G_b - \rho\varepsilon \tag{8}$$

and

$$u\frac{\partial \varepsilon}{\partial r} + v\frac{\partial \varepsilon}{\partial y} = \frac{\partial}{\partial r}\left[\left(\theta + \frac{\theta_t}{\sigma_\varepsilon}\right)\frac{\partial \varepsilon}{\partial r}\right] + \frac{\partial}{\partial y}\left[\left(\theta + \frac{\theta_t}{\sigma_\varepsilon}\right)\frac{\partial \varepsilon}{\partial y}\right] + C_1\frac{\varepsilon}{k}G_k - \rho C_2\frac{\varepsilon^2}{k} \tag{9}$$

The turbulent viscosity in the SKE model can be described by

$$\theta_t = C_\mu \frac{k^2}{\varepsilon} \tag{10}$$

The dimensionless empirical constants are given the standard values suggested by Rodi (1980): $C_\mu = 0.09$; $C_1 = 1.44$; $C_2 = 1.92$; $\sigma_k = 1.0$; and $\sigma_\varepsilon = 1.3$.

The solids transport equation in the model is included by user-defined function, and is

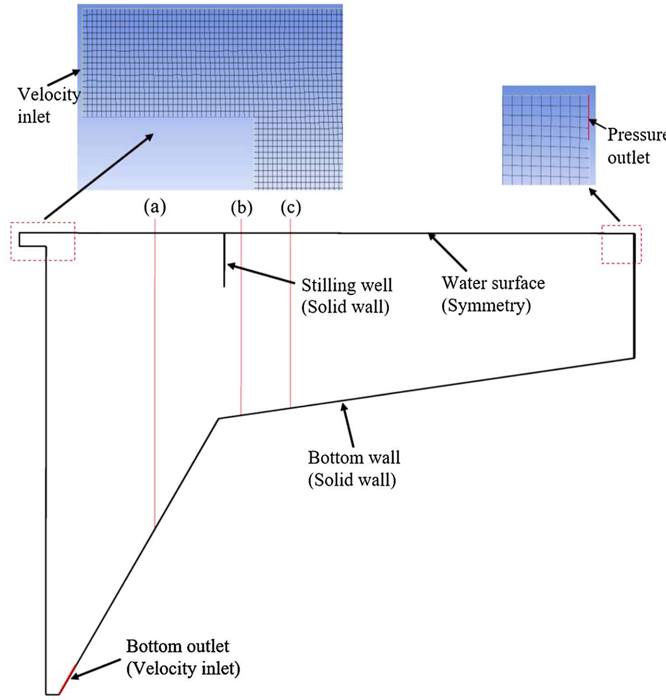

Fig. 1. Original SST diagram with representative computed locations and boundary conditions for Trial 1: (a–c) the radial locations for the model calibration shown in Fig. 3.

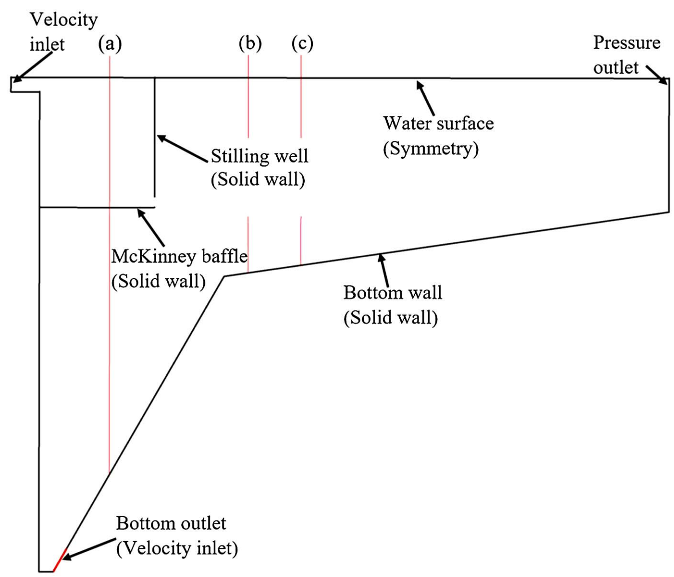

Fig. 2. Modified SST diagram with representative computed locations and boundary conditions for Trials 2 and 3: (a–c) the radial locations for the model calibration shown in Fig. 3.

Table 2. Inputs for the trials in this study

	Inflow parameters			Settling parameters			Dry solids density
Trial number	MLSS (g/L)	RAS ratio	Q_{in} (m^3/s)	V_o (m/h)	r_h (L/g)	r_p (L/g)	ρ_p (kg/m^3)
1	4.187	1.09	0.0506	12.64	0.340	3.4–30	1,000–2,100
2	3.384	1.09	0.0506	13.32	0.386	3.8–30	1,000–2,100
3	2.904	0.83	0.0900	13.32	0.386	3.8–30	1,000–2,100

J. Environ. Eng., 2020, 146(5): 04020028

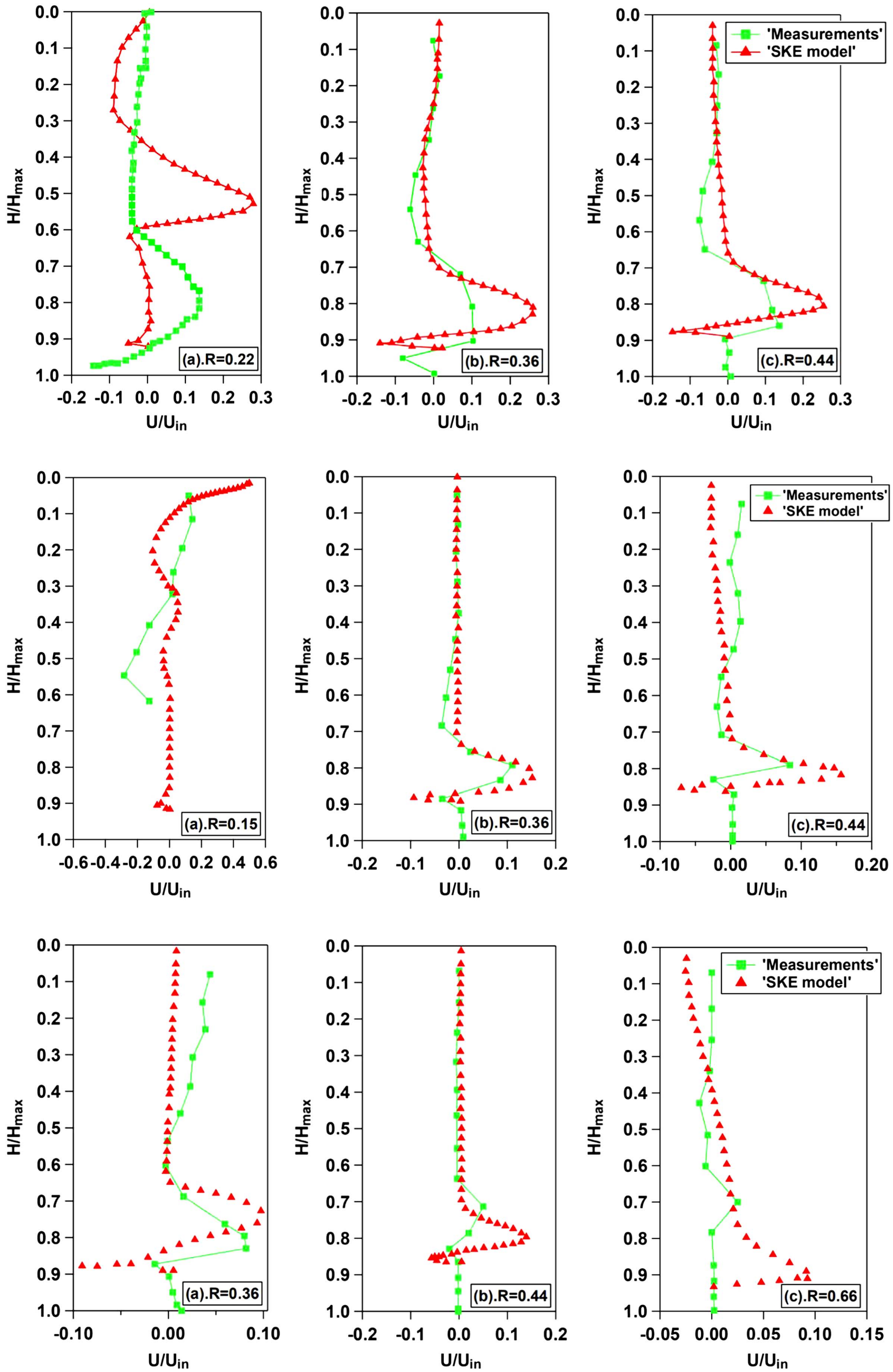

Fig. 3. Comparisons of radial velocity profiles (m/s) between the model predictions and field measurements for Trials 1–3, respectively. R is the ratio between the radial distance of the vertical measurement location to the radius of tank. Trial 1 (first row), Trial 2 (second row), Trial 3 (third row). The profiles of R = 0.22 for Trial 1 and R = 0.15 for Trial 2 are inside the stilling well. The other seven profiles are outside the stilling well.

$$u\frac{\partial C}{\partial r}+v\frac{\partial C}{\partial y}=\frac{1}{r}\frac{\partial}{\partial r}\left[r\left(\theta+\frac{\theta_t}{\sigma_r}\right)\frac{\partial C}{\partial r}\right]+\frac{1}{r}\frac{\partial}{\partial y}\left[r\left(\theta+\frac{\theta_t}{\sigma_y}\right)\frac{\partial C}{\partial y}-rV_sC\right] \quad (11)$$

where C = concentration of SS; θ = viscosity of the sludge mixture; θ_t = turbulent eddy viscosity; σ_r and σ_y = turbulent Schmidt numbers in the r and y directions, respectively (both are assumed to be 0.7 in this study); and V_s = solids settling velocity.

The solids rheological model is proposed by Bokil (1972) as

$$v = 1\times 10^{-6}e^{1.386C} \quad \text{for } C \le 1 \text{ g/L}$$

and

$$v = 2.9\times 10^{-6}e^{0.322C} \quad \text{for } C \ge 1 \text{ g/L} \quad (12)$$

where C = concentration of SS.

Velocity inlet boundary condition is applied to inlet and sludge bottom boundaries, which assumes a uniform distribution of all the dependent variables at the boundary face. For the surface outlet, a pressure outlet boundary condition is applied. Using this type of boundary condition, all flow quantities at the outlets are extrapolated from the interior domain. For the free ambient water surface, the rigid-lid approximation for all velocity components with full slip shear condition is assumed (Wang et al. 2008; Tarpagkou and Pantokratoras 2013); the free surface boundary is treated as a symmetry condition. The solid boundaries are specified as stationary walls with a no slip-shear condition, and a standard wall function is used with the turbulence models.

Geometry and Meshing

The general geometries of original and modified Witney SSTs (Burt 2010) and computational meshes with a nearly uniform cell size of 0.00625 × 0.00625 m and approximately 900,000 cells are shown in Figs. 1 and 2, respectively. The radius of the Witney SST is 18.3 m with a 1.8-m minimum side water depth. The tank floor slope and hopper floor slope are 7.5% and 60%, respectively. Gao and Stenstrom (2018a, 2019b) showed the results of mesh-independent tests for the original and modified SSTs, respectively. Because the surface outlet is extremely small compared with the inlet, the meshes near the surface outlet are enlarged in the figure to show the outlet meshes more clearly.

Model Verification

Three different trials were compared using Burt (2010) data for two different SSTs at the Witney WWTP for the model calibration. Trial 1 used the original SST with a large stilling well; Trials 2 and 3 are tested in a modified SST with the addition of a McKinney baffle below the stilling well. The baffle was added in anticipation of improving ESS, even at higher flow rates. The main inputs for these three trials are shown in Table 2. Fig. 3 shows the comparison between numerical velocity profiles and the corresponding experimental data. The figures shown from first row to the third row refer to the comparisons for Trials 1 to 3. Additionally, the first figure for Trial 1 shows the comparison inside the stilling well, while the other eight figures show the comparison outside the stilling well. Fig. 3 shows

Table 3. Effects of model parameters accounting for the particle with poor settling property in the Takács settling model settling (r_p), dry solids density (ρ_p), and turbulence specification methods on the inlet boundary condition on the performance indicators

	Geometries	Original SST			Modified SST					
	Trials	No. 1			No. 2			No. 3		
Exp. number	Model uncertainties	ESS (mg/L)	SBH (m)	RAS (mg/L)	ESS (mg/L)	SBH (m)	RAS (mg/L)	ESS (mg/L)	SBH (m)	RAS (mg/L)
Measurement		24.0	1.85	—	15.0	2.10	—	22.0	1.80	—
					r_p (L/g)					
1	3.40[a]/3.86[a]	**18.0**	1.90	7,790	**32.4**	1.90	6,366	**51.4**	1.85	5,800
2	8.00	**16.8**	1.93	7,800	**19.6**	1.92	6,280	**28.0**	1.85	5,825
3	12.25[a]/13.00[a]	**14.6**	2.01	7,798	**16.1**	1.95	6,482	**22.0**	1.85	6,230
4	20.00	**13.6**	2.00	7,830	**13.3**	2.03	6,378	**16.4**	1.85	5,820
5	30.00	**13.6**	2.04	7,800	**11.7**	1.96	6,455	**13.5**	1.85	5,823
Difference (%)[b]		**24.4**	6.87	0.5	**63.9**	6.40	3.11	**73.7**	0	6.50
					ρ_p (kg/m^3)					
6	1,000	*2,400*	*0.00*	*5,197*	*3,329*	*0.01*	*4,388*	*2,542*	*0.00*	*3,253*
7	1,100	**18.4**	2.00	7,835	**13.8**	1.98	6,483	**24.0**	1.86	5,848
8	1,450	**14.6**	2.01	7,798	**16.1**	1.95	6,482	**22.0**	1.85	6,230
9	1,800	**10.6**	2.20	7,800	**16.0**	1.93	6,468	**21.2**	1.85	5,812
10	2,100	**13.8**	2.12	7,789	**15.8**	1.93	6,438	**21.2**	1.85	5,809
Difference (%)[b]		**42.4**	9.10	5.87	**14.3**	2.53	0.69	**11.7**	0.53	6.76
					Inlet boundary					
11	No. 14[c]	14.6	2.01	7,848	16.2	1.96	6,532	21.8	1.85	5,843
12	No. 15[c]	14.6	2.01	7,804	16.4	1.95	6,483	21.5	1.85	5,834
13	No. 16[c]	14.6	2.01	7,798	16.1	1.95	6,482	22.0	1.85	6,230
Difference (%)[b]		0	0	0.63	1.22	0.51	0.77	2.27	0	6.36

Note: SBH = vertical distance from the top effluent to the location with 850 mg/L sludge concentration, which is the same definition applied in the Burt (2010). Values shown in italic font are results of the performance indicators with neutral density condition in each trial. Bond values are the results of the performance indicator, which is greatly influenced (more than 10% difference between the smallest and the largest value) by the sensitivity tests in each trial.
[a]Trials 1–3, respectively: 3.40 is 10 times the value of $\boldsymbol{r_h}$ (0.34 L/g) used in Trial 1, and 3.86 is 10 times the value of r_h (0.386 L/g) used in Trials 2 and 3. Also, 12.25 is the value of r_p used in Trial 1 in the original literature, and 13.00 is the value of r_p used in Trials 2 and 3 in the original literature.
[b]Percentage reduction between the maximum and minimum value of the performance indicator as the variation of the value of each model uncertainty.
[c]Rows numbered 14–16 from Table 1, respectively.

that the overall stream curvatures outside of the stilling well are reasonably predicted, but less well predicted inside the stilling well.

Results and Discussion

To evaluate the effects of the turbulence specification methods of the inlet boundary conditions and the values of the parameters r_p and ρ_p, sensitivity tests were conducted for different turbulence specifications and parameter values. Table 1 shows the parameter ranges used by previous researchers. Based upon these ranges, simulations were made from $r_p = 3.4$ to 30 L/g for Trial 1 and 3.86 to 30 L/g for Trials 2 and 3. Also, ρ_p was varied from 1,100 to 2,100 kg/m^3 for all trials. The field measurements and the predictions of each model for the performance indicators (SBH, ESS, and RAS concentrations) are summarized in Table 3.

Additionally, the neutral density condition was simulated to compare with the results of density-coupled conditions for each trial. All the parameter values and turbulence specification methods are summarized in the second column in Table 3.

Effects of Sludge Settling Parameter (r_p)

The settling velocity curves with varied r_p are shown in Fig. 4. The value of r_p controls the settling velocity with small particles (for concentration < 1.0 g/L), which shows an exponential increase, finally reaching a maximum. The peak settling velocity increases more than 30% as r_p increases from 3.4 to 30 L/g.

The field measurements and the predictions of each model for the performance indicators (SBH, ESS, and RAS concentrations) are summarized in Table 3. The simulations were selected based on the data available from Witney, which included observations at three different flow rates with and without the McKinney baffle. Fig. 3 shows the deviation between the measured ESS, which is a constant value under a certain flow condition, and the predicted ESS, which is affected by the r_p. The field measurements show that the ESS is acceptable for all three trials, although the ESS for Trial 2 is somewhat less. Trials 1 differs from Trials 2 and 3 because of the addition of the McKinney baffle for Trials 2 and 3. The flow rates are the same in Trials 1 and 2, but the mixed liquor suspended solids (MLSS) concentration is approximately 20% less in Trial 2. Also, the flow rate in Trial 3 is 80% larger than in Trial 1. The McKinney baffle is the primary reason for the improved performance of Trials 2 and 3 over Trial 1. Unfortunately, there are no observations for ESS at this higher flow without the McKinney baffle.

Model predictions for Trial 1 are always better than actual performance and are insensitive to r_p. Trials 2 and 3 are much more sensitive to r_p and predict failure due to high ESS at low values of r_p, even when the field observations show success. As r_p increases (better settling performance for small particles), ESS is reduced in each trial but especially in Trials 2 and 3, as shown in Fig. 5. The variation of the ESS with respect to r_p is large and causes remarkably different ESS predictions, even to the extent of predicting clarification failure (ESS > 30 mg/L). However, Table 3 shows that r_p has little influence on sludge thickening, and its effects on thickening are not likely to be important.

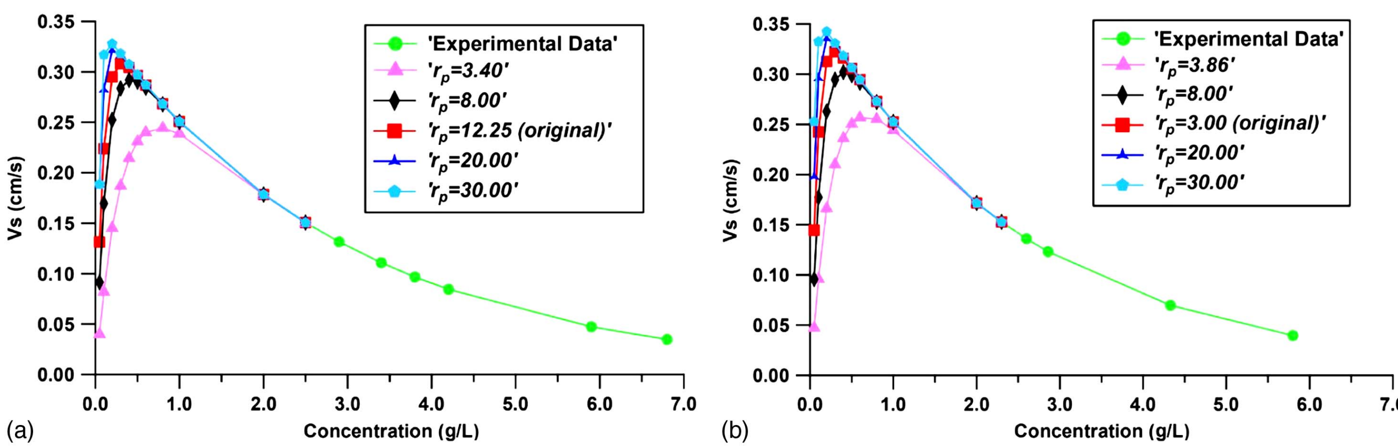

Fig. 4. Settling velocity curves with the variation of r_p: (a) Trial 1; and (b) Trials 2 and 3.

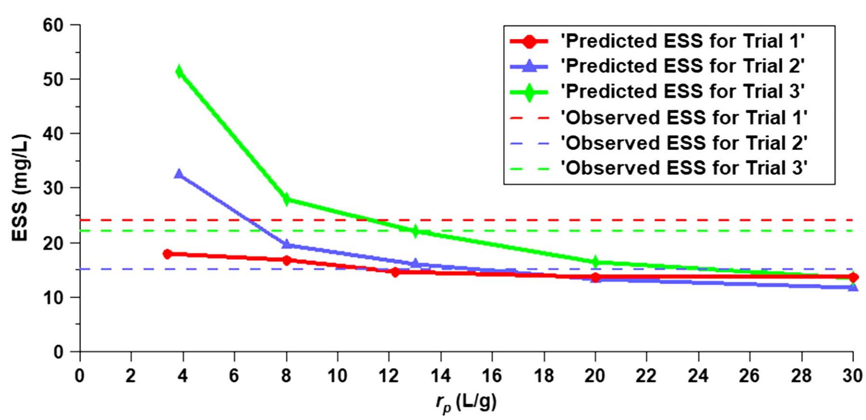

Fig. 5. Predictions of ESS (mg/L) with respect to r_p (L/g) for Trials 1–3.

The results in Fig. 5 show that comparison to field data is required for Trials 2 and 3, and that Trial 1 simulation is independent of field observations. Without field measurements for Trials 1 and 2, selecting the wrong value of r_p can lead to the opposite conclusion, where the model predicts that the original SST performs better than the modified SST. Selecting too large a value of r_p may significantly overpredict the clarification performance of the SST. Therefore, r_p should be well calibrated based on the predictions of the ESS and field measurements of multiple SSTs, not only to fulfill the calibration for each SST, but also to show the correct performance difference among the SSTs.

Figs. 6(a and b) show the predictions of settling velocity profiles for Trial 3 with the smallest and the largest values of r_p [(a) $r_p = 3.86$ and (b) 30 L/g, respectively]. It shows that the prediction of settling velocity for $r_p = 30$ L/g is higher than the prediction for $r_p = 3.86$ L/g in the entire main settling zone (circled in

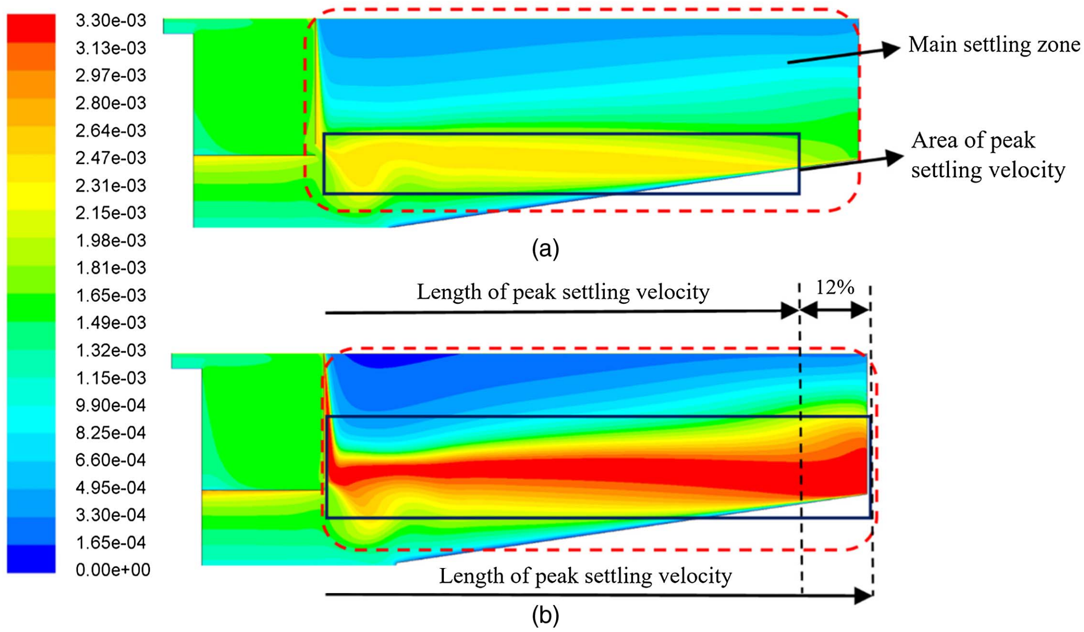

Fig. 6. Predictions of settling velocity profiles (m/s) for the Trial 3: (a) $r_p = 3.86$ L/g; and (b) $r_p = 30$ L/g.

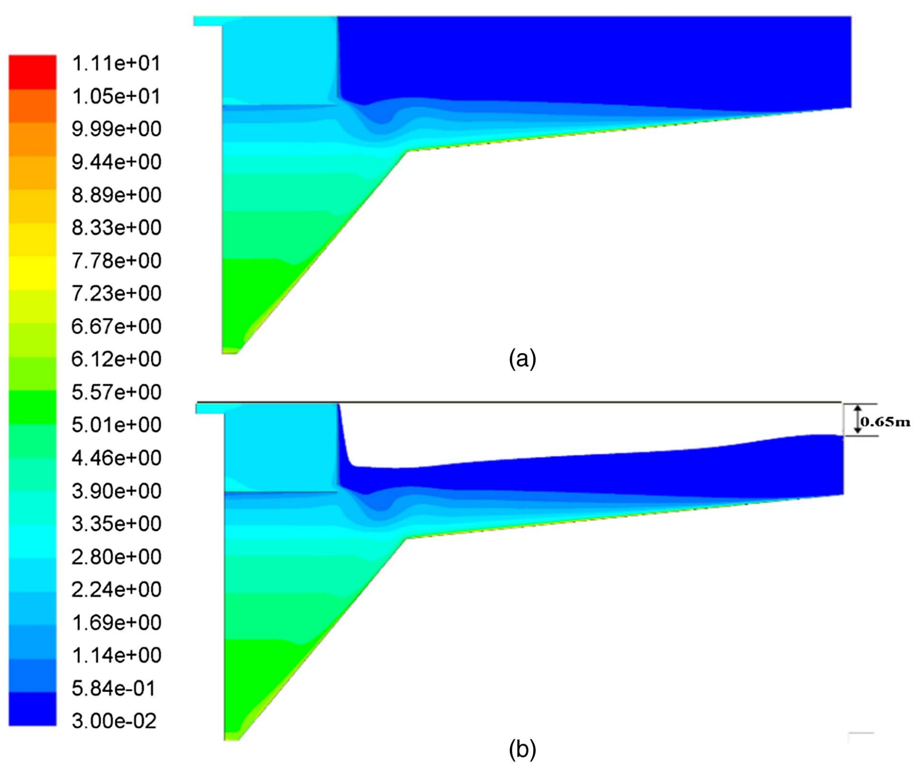

Fig. 7. Predictions of sludge concentration profiles (g/L) for Trial 3: (a) $r_p = 3.86$ L/g; and (b) $r_p = 30$ L/g. Only the regions with sludge concentration higher than 30 mg/L are shown.

dashed line).This difference becomes more significant near the side wall, where the settling velocity is one order of magnitude greater. Additionally, the region of the peak settling velocity (circled in black solid line) in Fig. 6(b) is 12% longer in the radial direction and 50% larger in overall size than that in Fig. 6(a). With greater sludge settling velocity (higher r_p value), the region of peak settling velocity exists in the entire main settling zone (from the stilling well to the side wall).

Figs. 7(a and b) show the prediction of sludge concentration profiles for Trial 3 with the smallest and the largest values of r_p [(a) $r_p = 3.86$; and (b) 30 L/g, respectively]. Only the regions with sludge concentration higher than 30 mg/L are shown. Fig. 7(b) shows that with larger r_p, the higher settling velocity in the main settling zone results in a lower suspended solids concentration at the upper region of the main settling zone. The 30 mg/L iso-concentration contour is 0.65 m below the water surface on the side wall. In contrast, the concentration profile predicted with small r_p [Fig. 7(a)] shows that the sludge concentration is above 30 mg/L in the entire SST.

Effects of Dry Solids Density (ρ_p)

Table 3 shows that, as the value of ρ_p increases in Trials 1 to 3, the predictions of ESS by the density-coupled model are reduced by 42.4%, 14.3%, and 11.7%, respectively. However, compared with the absolute difference between the smallest and the largest ESS

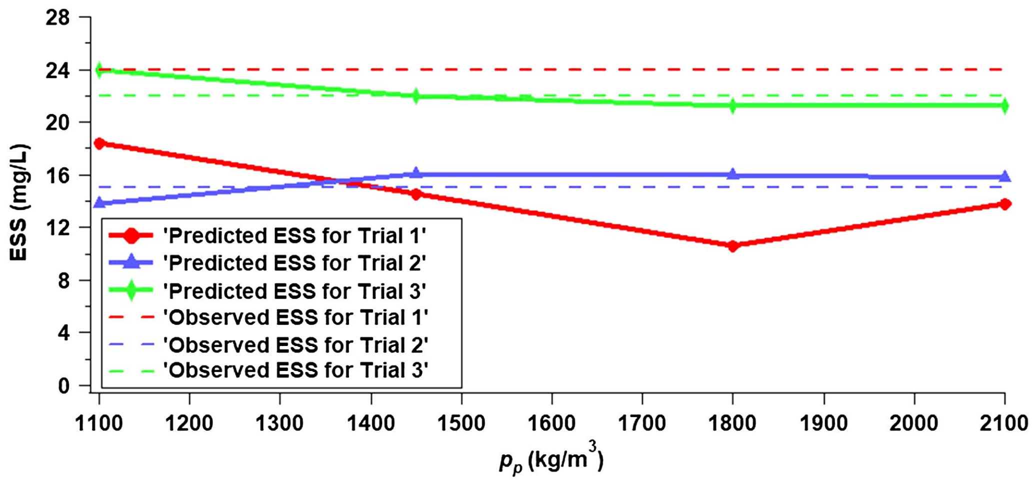

Fig. 8. Prediction of ESS (mg/L) respect to ρ_p (kg/m^3) for Trials 1–3.

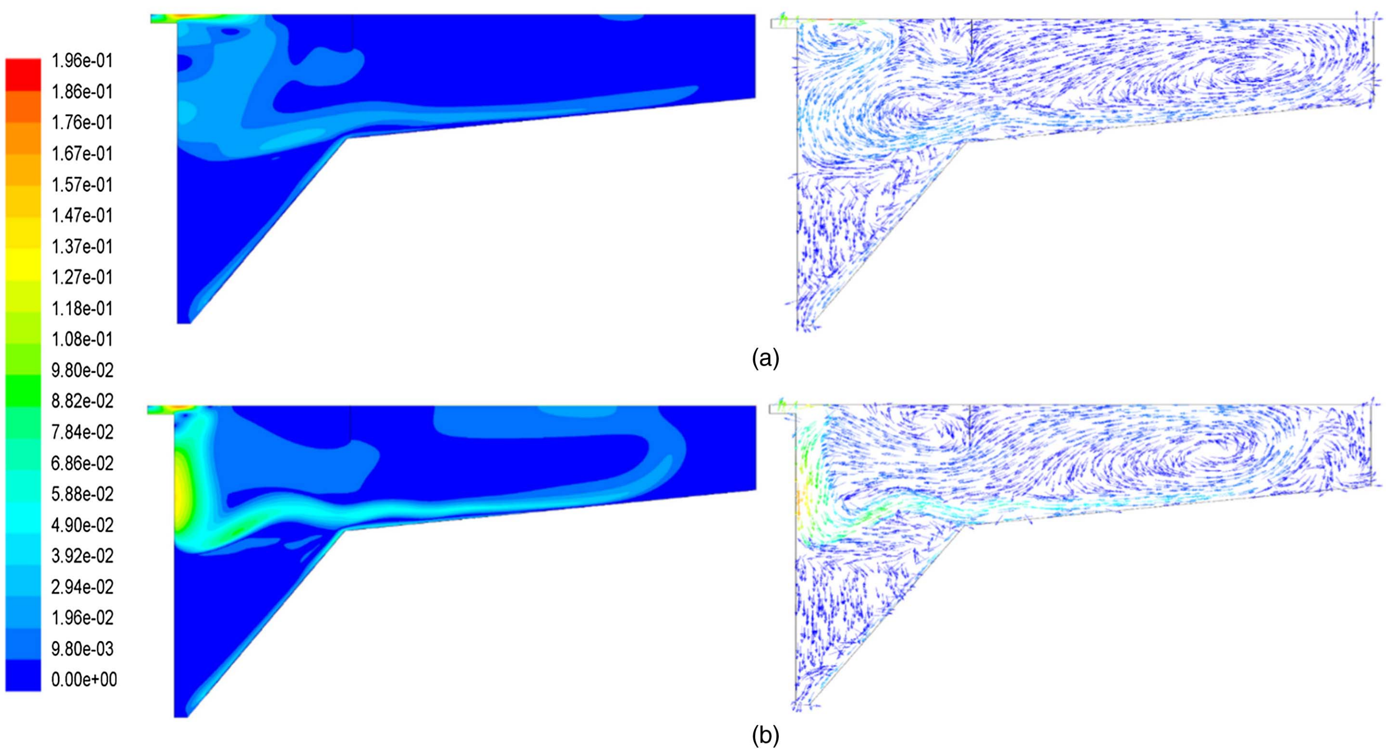

Fig. 9. Predictions of velocity magnitude and vector profiles (m/s) with two different dry solids densities for Trial 1: (a) 1,100 kg/m^3; and (b) 2,100 kg/m^3.

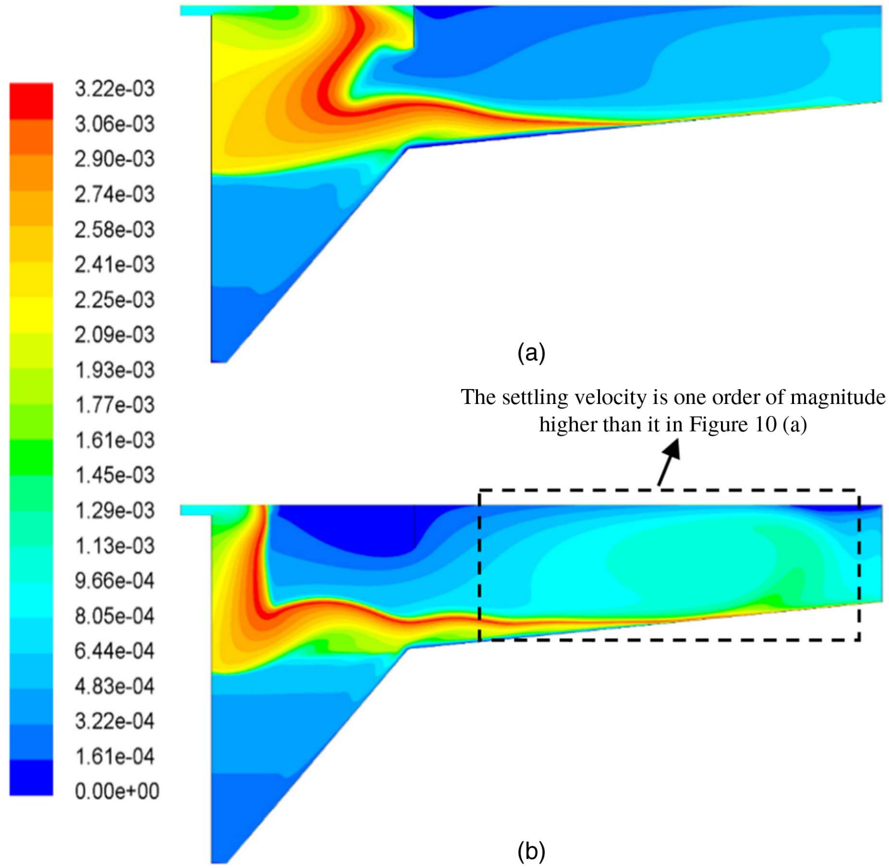

Fig. 10. Predictions of sludge settling velocity magnitude profiles (m/s) with two different dry solids densities for Trial 1: (a) 1,100 kg/m^3; and (b) 2,100 kg/m^3.

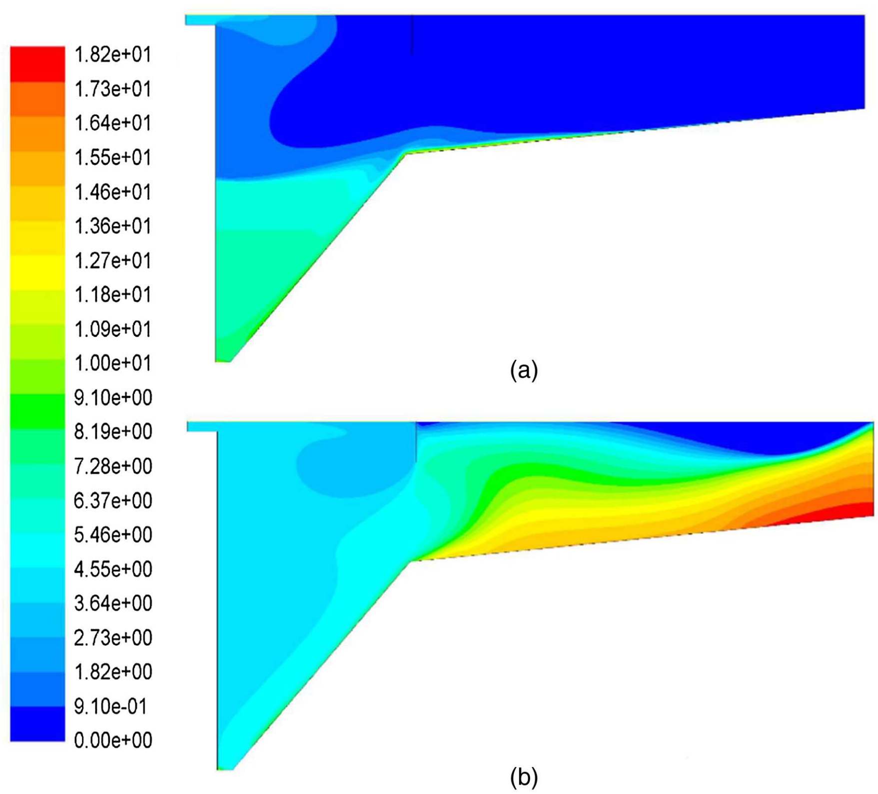

Fig. 11. Comparison of sludge concentration profiles (g/L) predicted by: (a) density-coupled condition; and (b) neutral density condition.

Table 4. Calculation of initial TKE and TDR with different turbulence specification methods on the inlet boundary condition and the averaged TKE and TDR on the scale of the entire SST

Number	Trial 1				Trial 2				Trial 3			
	Inlet boundary values		Averaged values		Inlet boundary values		Averaged values		Inlet boundary values		Averaged values	
	TKE	TDR	TKE	TDR	TKE	TDR	TKE	TDR	TKE	TDR	TKE	TDR
14[a]	7.60×10^{-4}	5.75×10^{-6}	5.40×10^{-5}	3.80×10^{-6}	7.60×10^{-4}	8.62×10^{-6}	4.38×10^{-5}	2.58×10^{-6}	2.41×10^{-3}	4.85×10^{-5}	9.44×10^{-5}	9.78×10^{-6}
15[a]	2.03×10^{-4}	1.67×10^{-3}	5.37×10^{-5}	3.69×10^{-6}	2.03×10^{-4}	1.67×10^{-3}	3.28×10^{-5}	2.28×10^{-6}	6.42×10^{-3}	9.38×10^{-3}	7.42×10^{-5}	8.62×10^{-6}
16[a]	3.80×10^{-5}	6.88×10^{-7}	5.21×10^{-5}	3.45×10^{-6}	3.75×10^{-5}	6.74×10^{-7}	3.46×10^{-5}	2.13×10^{-6}	1.20×10^{-4}	3.87×10^{-6}	7.90×10^{-5}	8.46×10^{-6}

[a]Rows numbered 14–16 are from Table 1.

predicted by different values of r_p as shown in Fig. 8, the variation of dry solids density still predicts the ESS value in an acceptable range, even if the value of solids density is almost doubled. Similar to the results of varying r_p, the change in the value of ρ_p in the density-coupled condition has little influence on the sludge thickening performance (SBH and RAS concentration). Therefore, a medium value of ρ_p, such as $1{,}450\ \mathrm{kg/m^3}$, is a good assumption.

Figs. 9(a and b) and 10(a and b) show the predictions of velocity and sludge settling velocity profiles with two different dry solids densities [(a) $1{,}100\ \mathrm{kg/m^3}$; and (b) $2{,}100\ \mathrm{kg/m^3}$] for Trial 1. The prediction of velocity profile with lower dry solids density [Fig. 9(a)] shows that the stronger initial momentum from the inlet results in a longer horizontal jet at the water surface. Along the horizontal jet, the velocity is gradually reduced as the energy is dissipated. At the same time, the sludge settling velocity [Fig. 10(a)] gradually increases along the horizontal jet and reaches a maximum at the end of the jet. Conversely, the prediction of velocity profile with higher dry solids density [Fig. 9(b)] shows a shorter horizontal jet, but a stronger density current in the vertical direction. Therefore, Fig. 10(b) shows that the peak sludge settling velocity is closer to the inlet location. Additionally, at the center of the main settling zone, the settling velocity with higher dry solids density is one order of magnitude higher than with a lower dry solids density, which leads to better clarification at the upper layer.

If the solids density is ignored (e.g., the neutral density condition), the SBH reaches the effluent weir and the ESS is dramatically overpredicted. Figs. 11(a and b) compare the sludge concentration profiles predicted by the density-coupled condition and neutral density condition, respectively. Compared with the density-coupled condition, which correctly predicts the sludge thickening at the bottom and clarification at the upper layer, the neutral density condition fails to predict sludge distribution correctly. Therefore, the hydrodynamics of SSTs should be predicted using density-coupled conditions.

Effects of Inlet-Turbulence Specification Methods

Table 1 (rows 14–16) shows the three different commonly used turbulence specification methods for the inlet boundary condition. The calculations of the initial TKE and TDR at the inlet for the three trials are shown in Table 4 under the inlet boundary values columns. The calculations of the averaged TKE and TDR on the scale of entire SST for the three trials are shown in Table 4 under the averaged values columns. The results in Table 4 show that, although the differences in the initial values of TKE and TDR calculated using the different specification methods can differ by as much as one to four orders of magnitude, respectively, the difference in the turbulence field calculated by the different boundary specification methods on the scale of the entire SST is negligible. Table 3 also shows that the difference of each performance indicator predicted by these three different turbulence specification methods is minimal. Hence, the different turbulence specification methods can only cause local effects in the near area of inlet boundary, and have few effects on the prediction of variables outside of the inlet zone.

Conclusions

In this study, a Fluent-based 2D SST model was used to analyze the impacts of using three different turbulence specification methods for the inlet boundary condition and ranges of two model parameters: (1) exponential term accounting for the small particle settling (r_p) in the Takács settling model, and (2) dry solids density (ρ_p) in the density-coupled conditions. Sensitivity tests were conducted to compare the predictions of the performance indicators (ESS, RAS, and SBH) and different variable fields (sludge settling velocity, velocity, and sludge concentration fields). The effects of the neutral density condition were also studied, and the prediction results were compared with the density-coupled results.

Based on the simulation results of the sensitivity tests, the following conclusions are made:

- The exponential term accounting for the small particle (r_p) in the Takács settling model is one of the key parameters to correctly predict the ESS. The small values of r_p may incorrectly predict the clarification failure of the SST, when the field measurements show that the SST is functioning well. However, r_p has little influence on sludge thickening. Therefore, r_p can be used to adjust the ESS, when SBH and RAS concentration are well calibrated to the field data, but the ESS does not fit field observations.
- The field observations show that the modified SST with the addition of a McKinney baffle performs better than the original SST, whereas using an incorrect value of r_p may result in the opposite prediction.
- It is recommended that r_p be adjusted to conform to ESS field measurements at multiple SSTs, not only to satisfy the calibration of ESS for each SST, but also to show the correct performance difference among the SSTs.
- The dry solids density (ρ_p) also has effects on the prediction of ESS, but the effects are small, compared with the effects of r_p, on predicted ESS. Doubling the value of ρ_p still produces acceptable comparisons to field data. Therefore, a medium value of r_p, such as 1,450 kg/m^3, is a good assumption.
- Because inflow to the SST is driven by density, using neutral density assumptions in the SST model can cause the wrong prediction for the SST performance.
- Different turbulence specification methods for the inlet boundary have only local effects on the hydrodynamics near the inlet, and have little influence on the prediction of the overall performance of the SST. Therefore, each turbulence specification method can be applied to obtain similar predictions.

Data Availability Statement

All data, models, and code generated or used during the study appear in the published article.

References

Bokil, S. D. 1972. "Effect of mechanical blending on the aerobic digestion of the waste activated sludge." Ph.D. thesis, Dept. of Civil and Engineering, Univ. of Windsor.

Bürger, R., S. Diehl, and I. Nopens. 2011. "A consistent modelling methodology for secondary settling tanks in wastewater treatment." *Water Res.* 45 (6): 2247–2260. https://doi.org/10.1016/j.watres.2011.01.020.

Burt, D. J. 2010. "Improved design of settling tanks using an extended drift flux model." Ph.D. thesis, Dept. of Mechanical Engineering, Univ. of Bristol.

Daigger, G. T. 1995. "Development of refined clarifier operating diagrams using an updated settling characteristics database." *Water Environ. Res.* 67 (1): 95–100. https://doi.org/10.2175/106143095X131231.

Das, S., H. Bai, C. Wu, J. H. Kao, B. Barney, M. Kidd, and M. Kuettel. 2016. "Improving the performance of industrial clarifiers using three-dimensional computational fluid dynamics." *Eng. Appl. Comput. Fluid Mech.* 10 (1): 130–144. https://doi.org/10.1080/19942060.2015.1121518.

Deininger, A., E. Holthausen, and P. A. Wilderer. 1998. "Velocity and solids distribution in circular secondary clarifiers: Full scale measurements and numerical modelling." *Water Res.* 32 (10): 2951–2958. https://doi.org/10.1016/S0043-1354(98)00072-4.

Ekama, G. A., J. L. Barnard, F. W. Gunthert, P. Krebs, J. A. McCorquodale, and E. J. Parker. 1997. *Secondary settling tanks: Theory, modelling, design and operation*. London: IAWQ.

Ekama, G. A., and P. Marais. 2004. "Assessing the applicability of the 1D flux theory to full-scale secondary settling tank design with a 2D hydrodynamic model." *Water Res.* 38 (3): 495–506. https://doi.org/10.1016/j.watres.2003.10.026.

Gao, H., and M. K. Stenstrom. 2017. "Computational fluid dynamics applied to secondary clarifier analysis." In *Proc., World Environmental and Water Resources Congress 2017: Water, Wastewater, and Stormwater, Urban Watershed Management, and Municipal Water Infrastructure*, edited by C. N. Dunn and B. VanWeele, 301–315. Reston, VA: ASCE. https://doi.org/10.1061/9780784480632.

Gao, H., and M. K. Stenstrom. 2018a. "Evaluation of three turbulence models in predicting of the hydrodynamics of a secondary sedimentation tank." *Water Res.* 143 (Oct): 445–456. https://doi.org/10.1016/j.watres.2018.06.067.

Gao, H., and M. K. Stenstrom. 2018b. "Turbulence and inter-phase mass diffusion assumptions on performance of secondary settling tanks." *Water Environ. Res.* 91 (2): 101–110. https://doi.org/10.1002/wer.1003.

Gao, H., and M. K. Stenstrom. 2019a. "Evaluating the effects of inlet geometry on the flux capacity of secondary settling tanks with computational fluid dynamics model and one-dimensional flux theory model." *J. Environ. Eng.* 145 (10): 04019065. https://doi.org/10.1061/(ASCE)EE.1943-7870.0001582.

Gao, H., and M. K. Stenstrom. 2019b. "Generalizing the effects of the baffling structures on the buoyancy-induced turbulence in secondary settling tanks with eleven different geometries using CFD models." *Chem. Eng. Res. Des.* 143 (Mar): 215–225. https://doi.org/10.1016/j.cherd.2019.01.015.

Gao, H., and M. K. Stenstrom. 2019c. "The influence of wind in secondary settling tanks for wastewater treatment—A computational fluid dynamics study. I: Circular secondary settling tanks." *Water Environ. Res.* https://doi.org/10.1002/wer.1241.

Gao, H., and M. K. Stenstrom. 2019d. "The influence of wind in secondary settling tanks for wastewater treatment—A computational fluid dynamics study. II: Rectangular secondary settling tanks." *Water Environ. Res.* https://doi.org/10.1002/wer.1244.

Griborio, A., and J. A. McCorquodale. 2016. "Lessons learned from 10 years of clarifier CFD modeling: The 2Dc experience." In *Proc., 89th Annual Water Environment Federation Technical Exhibition and Conf. (CD-ROM)*. Alexandria, VA: Water Environment Federation.

Guyonvarch, E., E. Ramin, M. Kulahci, and B. G. Plósz. 2015. "iCFD: Interpreted computational fluid dynamics-degeneration of CFD to one-dimensional advection-dispersion models using statistical experimental design: The secondary clarifier." *Water Res.* 83 (Oct): 396–411. https://doi.org/10.1016/j.watres.2015.06.012.

Kinnear, D. J. 2002. "Biological solids sedimentation: A model incorporating in fundamental settling parameters." Ph.D. thesis, Dept. of Civil and Environmental Engineering, Univ. of Utah.

Kleine, D., and B. D. Reddy. 2005. "Finite element analysis of flows in secondary settling tanks." *Int. J. Numer. Meth. Eng.* 64 (7): 849–876. https://doi.org/10.1002/nme.1373.

Krebs, P., A. Stamou, J. L. Garcia-Heras, and W. Rodi. 1996. "Influence of inlet and outlet configuration on the flow in secondary clarifiers." *Water Sci. Technol.* 34 (5–6): 1–9. https://doi.org/10.2166/wst.1996.0528.

Lakehal, D., P. Krebs, J. Krijgsman, and W. Rodi. 1999. "Computing shear flow and sludge blanket in secondary clarifiers." *J. Hydraul. Eng.* 125 (3): 253–262. https://doi.org/10.1061/(ASCE)0733-9429(1999)125:3(253).

Larsen, P. 1977. *On the hydraulics of rectangular settling basins: Experimental and theoretical studies*. Lund, Sweden: Dept. of Water Resources Engineering, Lund Institute of Technology.

Li, B., and M. K. Stenstrom. 2014. "Research advances and challenges in one-dimensional modeling of secondary settling tanks: A critical review." *Water Res.* 65 (Nov): 40–63. https://doi.org/10.1016/j.watres.2014.07.007.

McCorquodale, J. A., E. La Motta, A. Griborio, I. Georgiou, and J. Homes. 2004. *Development of software for modeling activated sludge clarifier system*. Technology Transfer Report Submitted to United States Environmental Protection Agency. New Orleans, LA: Schielder Urban Environmental System Center, Univ. of New Orleans.

Patziger, M. 2016. "Computational fluid dynamics investigation of shallow circular secondary settling tanks: Inlet geometry and performance indicators." *Chem. Eng. Res. Des.* 112 (Aug): 122–131. https://doi.org/10.1016/j.cherd.2016.06.018.

Patziger, M., H. Kainz, M. Hunze, and J. Jozsa. 2012. "Influence of secondary settling tank performance on suspended solids mass balance in activated sludge systems." *Water Res.* 46 (7): 2415–2424. https://doi.org/10.1016/j.watres.2012.02.007.

Plósz, B. G., I. Nopes, L. Rieger, A. Griborio, J. D. Clercq, P. A. Vanrolleghem, G. T. Daigger, I. Takács, J. Wicks, and G. A. Ekama. 2012. "A critical review of clarifier modelling: State of the art and engineering practices." In *Proc., WWTmod2012—3rd IWA/WEF Wastewater Treatment Modelling Seminar*, 27–30. Mont-Sainte-Anne, QC, Canada.

Ramin, E., D. S. Wagner, L. Yde, P. J. Binning, M. R. Rasmussen, P. S. Mikkelsen, and B. G. Plósz. 2014. "A new settling velocity model to describe secondary sedimentation." *Water Res.* 66 (Dec): 447–458. https://doi.org/10.1016/j.watres.2014.08.034.

Ratkovich, N., W. Horn, F. P. Helmus, S. Rosenberger, W. Naessens, I. Nopens, and T. R. Bentzen. 2013. "Activated sludge rheology: A critical review on data collection and modelling." *Water Res.* 47 (2): 463–482. https://doi.org/10.1016/j.watres.2012.11.021.

Rodi, W. 1980. *Turbulent models and their application in hydraulics: A state of the art review.* Delft, Netherlands: International Association for Hydraulics Research.

Saffarian, M. R., M. H. Hamedi, and M. Shams. 2010. "Comparison of various settling velocity functions and non-Newtonian fluid models in circular secondary clarifiers." *Korean J. Chem. Eng.* 27 (5): 1497–1508. https://doi.org/10.1007/s11814-010-0253-0.

Saffarian, M. R., M. H. Hamedi, and M. Shams. 2011. "Numerical simulation of a secondary clarifier in a sewage treatment plant using modified Bingham model." *Can. J. Civ. Eng.* 38 (1): 11–22. https://doi.org/10.1139/L10-106.

Samstag, R. W., J. A. McCorquodale, and S. P. Zhou. 1992. "Prospects for transport modeling of process tanks." *Water Sci. Technol.* 26 (5–6): 1401–1410. https://doi.org/10.2166/wst.1992.0583.

Takács, I., G. G. Patry, and D. Nolasco. 1991. "A dynamic model of the clarification-thickening process." *Water Res.* 25 (10): 1263–1271. https://doi.org/10.1016/0043-1354(91)90066-Y.

Tamayol, A., B. Firoozabadi, and M. A. Ashjari. 2009. "Hydrodynamics of secondary settling tanks and increasing their performance using baffles." *J. Environ. Eng.* 136 (1): 32–39. https://doi.org/10.1061/(ASCE)EE.1943-7870.0000126.

Tarpagkou, R., and A. Pantokratoras. 2013. "CFD methodology for sedimentation tanks: The effect of secondary phase on fluid phase using DPM coupled calculations." *Appl. Math. Model.* 37 (5): 3478–3494. https://doi.org/10.1016/j.apm.2012.08.011.

Vitasovic, Z. C., S. Zhou, J. A. McCorquodale, and K. Lingren. 1997. "Secondary clarifier analysis using data from the Clarifier Research Technical Committee protocol." *Water Environ. Res.* 69 (5): 999–1007. https://doi.org/10.2175/106143097X125696.

Wahlberg, E. J., and T. M. Keinath. 1988. "Development of settling flux curves using SVI." *Water Pollut. Control Fed.* 60 (12): 2095.

Wang, X., L. Yang, Y. Sun, L. Song, M. Zhang, and Y. Cao. 2008. "Three-dimensional simulation on the water flow field and suspended solids concentration in the rectangular sedimentation tank." *J. Environ. Eng.* 134 (11): 902–911. https://doi.org/10.1139/l92-044.

Weiss, M., B. G. Plósz, K. Essemiani, and J. Meinhold. 2007. "Suction-lift sludge removal and non-Newtonian flow behaviour in circular secondary clarifiers: Numerical modelling and measurements." *J. Chem. Eng.* 132 (1–3): 241–255. https://doi.org/10.1016/j.cej.2007.01.004.

Xanthos, S., M. Gong, K. Ramalingam, J. Fillos, A. Deur, K. Beckmann, and J. A. McCorquodale. 2011. "Performance assessment of secondary settling tanks using CFD modeling." *Water Resour. Manage.* 25 (4): 1169–1182. https://doi.org/10.1007/s11269-010-9620-1.

Xanthos, S., K. Ramalingam, S. Lipke, B. McKenna, and J. Fillos. 2013. "Implementation of CFD modeling in the performance assessment and optimization of secondary clarifiers: The PVSC case study." *Water Sci. Technol.* 68 (9): 1901–1913. https://doi.org/10.2166/wst.2013.280.

Xu, G., F. J. Yin, Y. J. Xu, and H. Q. Yu. 2017. "A force-based mechanistic model for describing activated sludge settling process." *Water Res.* 127 (Dec): 118–126. https://doi.org/10.1016/j.watres.2017.10.013.

Zhou, S., and J. A. McCorquodale. 1992a. "Influence of skirt radius on performance of circular clarifier with density stratification." *Int. J. Numer. Meth. Fluid.* 14 (8): 919–934. https://doi.org/10.1002/fld.1650140804.

Zhou, S., and J. A. McCorquodale. 1992b. "Mathematical modelling of a circular clarifier." *Can. J. Civ. Eng.* 19 (3): 365–374. https://doi.org/10.1139/l92-044.

Zhou, S., and J. A. McCorquodale. 1992c. "Modeling of rectangular settling tanks." *J. Hydraul. Eng.* 118 (10): 1391–1405. https://doi.org/10.1061/(ASCE)0733-9429(1992)118:10(1391).